A mesoporous silica nanosphere-based drug delivery system using an electrically conducting polymer

Nanotechnology **20** (2009) 275102 (12pp) doi:10.1088/0957-4484/20/27/275102

A mesoporous silica nanosphere-based drug delivery system using an electrically conducting polymer

Youngnam Cho[1], Riyi Shi[1,2], Albena Ivanisevic[2,3] and Richard Ben Borgens[1,2]

[1] Center for Paralysis Research, School of Veterinary Medicine, Purdue University, West Lafayette, IN 47907, USA
[2] Weldon School of Biomedical Engineering, Purdue University, West Lafayette, IN 47907, USA
[3] Department of Chemistry, Purdue University, West Lafayette, IN 47907, USA

E-mail: cho22@purdue.edu

Received 12 March 2009, in final form 15 May 2009
Published 16 June 2009
Online at stacks.iop.org/Nano/20/275102

Abstract

In this study, a mesoporous silica nanoparticle (MSN)-based nerve growth factor (NGF) delivery system has been successfully embedded within an electroactive polypyrrol (Ppy). The spherical particles with ∼100 nm diameter possess a large surface-to-volume ratio for the entrapment of NGF into the pores of MSNs while retaining their bioactivity. Direct incorporation of MSN-NGF within Ppy was achieved during electrochemical polymerization. The loading amount and release profile of NGF from the composite was investigated by sandwich ELISA. The NGF incorporation can be controllable by varying particle concentration or by extending electrodeposition time. The morphology and chemical composition of the Ppy/MSN-NGF composite was evaluated by atomic force microscopy (AFM), transmission electron microscopy (TEM), scanning electron microscopy (SEM), and x-ray photoelectron spectroscopy (XPS). Optical and electron microscopy revealed a characteristic attachment of PC 12 cells and the outgrowth of their neurites when grown on the Ppy/MSN-NGF composite as a result of a sustained and controlled release of NGF. In order to observe the effectiveness of electrical stimulation, neurite extension of cells cultured on unstimulated and stimulated Ppy/MSN-NGF was compared. The NGF release in the presence of electrical stimulation promoted significantly greater neurite extension.

(Some figures in this article are in colour only in the electronic version)

1. Introduction

Efforts to develop microfabricated neural devices using conducting electroactive polymers have been employed for application to the nervous system [1–5]. The possible therapeutic applications of such devices could be directly towards improving behavioral recovery. The natural extension of such an approach would consequently result in the development of brain-controlled devices, vision facilitation implants, nerve function modulators, and spinal cord stimulators to name a few [6–8]. However, unpredictable device failures, which might result from such things as undesirable scar tissue formation and mechanical mismatch between tissue and electrodes, present critical issues for possible chronic applications and could impede clinical development. As a result, current research on conducting polymer-based electrodes includes the integration of active chemical substances (e.g. drugs, nerve growth factors, neurotrophic factors, etc [9–12]). The goal is to incorporate biomolecules into the polymer site, where surface immobilization or electrochemical deposition as a dopant is the most commonly used method [13–17]. However, low encapsulation and rapid release of biomolecules associated with the limited surface area and inherent hydrophobic nature

of conductive polymers poses many challenges. In addition, electrochemical deposition using a solution composed of a biological entity and pyrrole monomers restrict homogeneous drug distribution throughout the polypyrrole surface and interfere with electrochemical control of various parameters such as film thickness, loading concentration, and diffusion of the biomolecules of interest. Consequently, complexity in the process as well as a decrease in conductivity associated with the surface density of immobilized peptides has encouraged us to search for an alternative method.

Site-specific drug delivery in the vicinity of a biomedical implant would enhance the performance of the incorporated drugs and also reduce the systemic exposure of those drugs, likely reducing or preventing toxicity and other unwanted side effects. Nanoparticles, as a reservoir of single or multiple substances, are capable of delivering highly concentrated chemical agents in a controlled-release manner [18–24]. Substantial efforts have been made to incorporate nanoparticles into the polymer matrix using electropolymerization. Most processes involve the attachment of electroactive polymer ligands (e.g. pyrrole-based monomers) to the surface of metal-nanoparticles—or the development of conductive polymer/metal-nanoparticle composites through the chemical reduction of the reactant metallic salts [25–29]. Such approaches encounter problems resulting from the assembly of particles on the surface, or the encapsulation of the drug entity. An intriguing further development involves the electrochemical assembly of drug-filled nanoparticles (e.g. metal, semiconductor, or insulator) within electroactive surfaces. A large surface-to-volume area and the well-defined internal structure of mesoporous silica nanoparticles (MSNs) make them ideal for adsorption and release of a variety of chemical substances. This might enhance drug loading capacity, and in addition, the hydrophilic properties of MSNs readily encourage attachment and spreading of cells. Moreover, the simplicity of fabrication additionally allows the composite to be integrated with conventional implantable biomedical devices that are already in clinical use.

As an electroactive conducting polymer, polypyrrole (Ppy) is the most widely studied class of conductive polymers due to its aqueous solubility, low oxidation potential, high conductivity, and biocompatibility with mammalian cells [30, 31]. Such versatile polymers can conduct current, simultaneously maintaining their inherent organic nature which is a crucial aspect for communicating with biosystems. Many efforts have been aimed at incorporating polypyrrole and/or its derivatives in biomedical applications by electrochemically entrapping a variety of anions and cations including growth factors, anti-inflammatory drugs, ATP, glutamate, and protonated dopamine [10, 32–34]. These dopants are carried inside the membrane and would be released through natural diffusion or external stimuli such as pH, temperature, or electrical stimulation.

In this study, we have optimized the synthesis and deposition of MSNs within a conductive polymer film—utilizing them as a neurotrophic factor (e.g. NGF) carrier to promote cell spreading and differentiation. The Ppy/MSN-NGF composite has several potential advantages in this regard: (i) the large surface area of the conducting polymer offers efficient loading of NGF-filled nanoparticles. Such a composite would be beneficial for co-delivery of a variety of drugs for multifunctional purposes, (ii) the nanoscaled surface created by selectively adapting particle functionality, arrangement, and size, enables control of surface chemistry as well as topography, (iii) such NGF-coated surfaces would be an excellent substrate for cellular attachment, adhesion, growth, and differentiation, and (iv) in the presence of electrical stimulation, the spontaneous and reversible oxidation/reduction reaction would promote neuronal survival and neurite outgrowth through NGF release from inside MSNs. Such an innovative and flexible tool might offer a promising strategy for further development of a particulated electroactive polymer surface. Furthermore this may be useful for organizing cellular behavior through the programmable localization of molecules based on electrical stimulation of the carrier.

2. Materials and methods

2.1. Synthesis of MSNs and loading of NGF into them

All chemicals were purchased from Sigma-Aldrich unless otherwise specified. MCM-41-type mesoporous silica nanoparticles (MSNs) were synthesized as previously described [35]. First, cetyltrimethylammonium bromide (CTAB) was dissolved in a solution of deionized water and ammonia. Subsequently, mesitylene was added as a pore-expanding agent. The mixture was stirred at 80 °C for 2 h followed by addition of tetraethyl orthosilicate (TEOS). The solutions were stirred vigorously at 80 °C until a white precipitate was formed. The resulting product was filtered, rinsed with water, and dried at 100 °C for 12 h. Finally, MSNs removed from the template materials were prepared by the acidic extraction method. For NGF immobilization, 5 ml of PBS solution with 100 μl of NGF 2.5 S (Invitrogen, 100 μg ml^{-1}) was stirred for 6 h at room temperature in the presence of 20 mg of dried MSN. The suspensions were centrifuged and dried overnight at room temperature under vacuum.

2.2. Characterization of particles

The surface properties of MSNs were analyzed by nitrogen adsorption/desorption measurements at −196 °C using an ASAP 2010 sorptometer (Micromeritics, USA). The Brunauer–Emmett–Teller (BET) and Barrett–Joyner–Halenda (BJH) methods were employed to calculate surface areas and pore volumes. The TEM examination was carried out to observe the morphology of MSNs before and after entrapment of NGF using a JEOL 2000FX. Particle size distribution was measured by dynamic light scattering (DLS).

2.3. The synthesis of polypyrrole incorporated with MSN-NGF

Polypyrrole (Ppy) was electrochemically prepared on indium tin oxide (ITO)-coated glass slides (Delta Technologies) using a 604 model potentiostat (CH Instruments). The three electrode cells contained working, counter, and reference

electrodes, where an ITO-coated borosilicate glass slide, a platinum gauze, and a saturated calomel electrode were employed, respectively. Individual ITO slides were cut into small pieces of 1×1 cm^2 and sonicated with acetone, methanol, and water. All solutions including pyrrole monomers were freshly prepared prior to use. We synthesized three different types of Ppy films using 0.1 M sodium salt of poly(styrene sulfonate) (PSS) as a dopant ion: Ppy, Ppy/MSN, and Ppy/MSN-NGF. To synthesize Ppy films, ITO films were immersed in an aqueous solution of 0.1 M pyrrole monomer and 0.1 M PSS by applying a suitable cathodic potential of 0.7 V. Ppy/MSN or Ppy/MSN-NGF was electrodeposited on ITO by first applying a potential of 0.7 V in a solution composed of 0.1 M pyrrole monomer, 0.1 M PSS for 2 s, and subsequently, a constant electrical potential (-1 to -3 V for 200 s) for MSN or MSN/NGF electrodeposition. The corresponding thickness for all films was approximately 1.3 μm. These films were immediately rinsed with deionized water and dried under nitrogen to avoid any further deposition.

2.4. Film thickness measurement

The thickness of the electrodeposited film was determined by averaging several measurements using an Alpha step 500 stylus profilometer. Ppy films were produced between 0.5–2.0 μm depending on the deposition time and the applied electrical potential. For the purpose of *in vitro* cell culture study, films with 0.5 μm thickness were fabricated where films with $\sim$1.5 μm thickness were usually employed for other surface characterization studies.

2.5. Atomic force microscopy (AFM) and scanning electron microscopy (SEM)

Surface morphology was characterized by AFM and SEM. AFM images were obtained using PSIA X-120 AFM to compare the surface roughness after electropolymerization. The experiments were performed in tapping mode using a PSIA non-contact cantilever with nominal spring constants of 42 N m^{-1} and a tip radius of 10 nm under ambient conditions. The image with a 5 μm $\times$ 5 μm scan size consisted of 256×256 points of height data and a scan rate of 1.0 Hz/line. Surface data from AFM was further processed with XEI software. The analyses of various types of Ppy films were performed on a FEI NOVA nanoSEM (FEI company) using a 5 kV acceleration voltage. Prior to these measurements, all samples were sputtered with gold–palladium. Cells on Ppy films were fixed in 2.5% glutaraldehyde, and dehydrated with increasing concentrations of ethanol by conventional methods. After drying, the cells were covered with gold ions in a JEOL JFC-110 ion sputtering (Tokyo, Japan) and analyzed in a JEOL JSM-840 SEM.

2.6. X-ray photoelectron spectroscopy (XPS)

Survey and high resolution XPS scans were collected with a Kratos Axis ULTRA x-ray photoelectron spectrometer. The instrument was equipped with a monochromatic Al Kα x-ray source, small area extraction optics, spherical capacitor electron energy analyzer, and a dual channel plate position sensitive detector. Survey spectra were taken from 0 to 1100 eV with a pass energy of 160 eV. High resolution scans were collected with a pass energy of 40 eV. Ppy films characterized by XPS confirmed the presence of MSNs and NGF immobilized within the pores of MSNs. Data analysis was performed using a commercial software package, Casa 2310, through fitting by Gaussian and Lorentzian functions. The high resolution data for C 1s, N 1s, Si 1s, and Si 2s were deconvoluted based on the peak area analysis, and then per cent assignments were made for the components under each element.

2.7. Characterization of Ppy/MSN-NGF composite

The direct conductivity of various types of Ppy films was measured using the four-probe technique on a SZ85 digital multimeter (Suzhou Telecommunication Factory China) at room temperature. When applying a constant current across the surface, the voltage was measured and further correlated to determine resistance. Using the Van der Pauw equation, the sheet conductivity of films was calculated. Measurements were performed four times in different directions from the center of the film. Cyclic voltammetry (CV) experiments were carried out using a 604 model potentiostat (CH instruments) at room temperature. In a three electrode cell, platinum gauze, a saturated silver/silver chloride, and functionalized Ppy film were used as counter, reference, and working electrodes respectively to observe the electrochemical properties of the surface.

2.8. The release profile of NGF from Ppy/MSN-NGF composite

The release behavior of NGF from Ppy/MSN-NGF composite was assessed using a commercially available sandwich ELISA kit (Millipore). The PBS solution containing Ppy/MSN-NGF was kept at 37 °C until an aliquot was taken from the suspension at different times. The aliquots collected were evaluated with ELISA immunoassay in undiluted aqueous samples. The intracellular NGF content was calculated based on the absorbance at 450 nm. Each NGF 'release' experiment was performed in triplicate.

2.9. PC 12 cell culture

PC 12 cells were seeded in Dulbecco's modified eagle's medium (DMEM; Invitrogen) supplemented with a density of 1×10^6 cells ml^{-1} in a medium containing 12.5% horse serum, 2.5% fetal bovine serum, 50 U ml^{-1} penicillin, and 5 mg ml^{-1} streptomycin at an incubator setting of 5% CO_2 and 37 °C. After trypsinization and centrifugation, cell pellets were resuspended in tissue culture dishes containing Ppy films to observe both the adhesion property and neurite extension as a function of time. During these experiments, PC 12 cells grown on bare Ppy substrate were supplied an appropriate amount of NGF solution (50 ng nl^{-1}) in medium whereas cells cultured on Ppy films with incorporation of NGF were maintained without any addition of NGF. Finally, the cells were

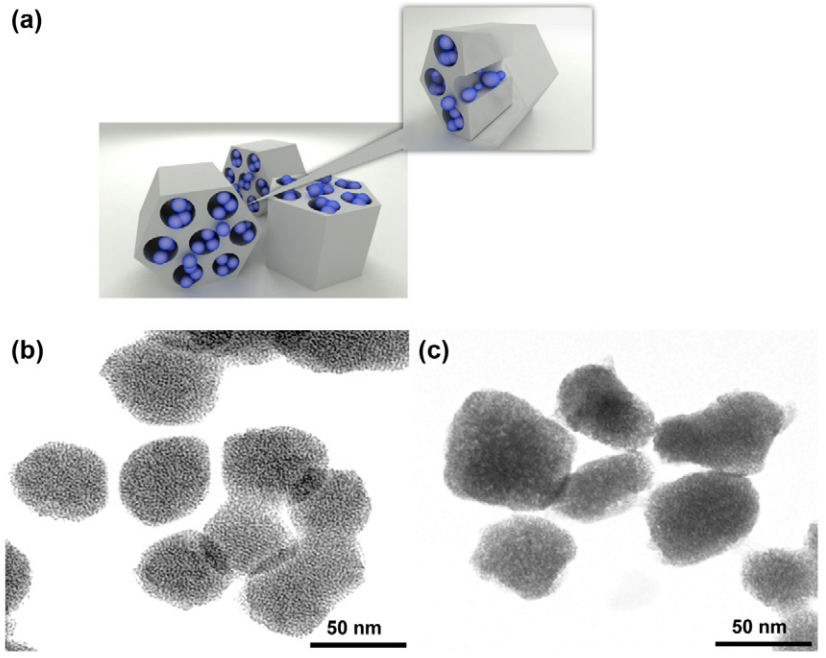

(d)

	S_{BET} (m^2/g)	W_{BJH} (nm)	V_t (cm^3/g)	Particle size (nm)	Amt of NGF loaded (%)
MSNs	1040	4.71	1.93	101 ± 15	—
MSN-NGF	401	2.04	0.22	125 ± 31	31.5

Figure 1. (a) Schematic representation of NGF-loaded MSNs. The incorporation of NGF (blue spheres) is based on the electrostatic interaction of electro-negative silica matrix and electro-positive NGF. The NGF is shown residing in the MCM-41-type mesoporous channels. (b) and (c) show TEM micrographs of large-pore MSNs before and after entrapment of NGF. The 'as-synthesized' MSNs show faintly visible hexagonally ordered parallel stripes, where NGF-filled MSNs clearly exhibit the presence of molecules on interior and exterior surface as represented by dots, or a pedunculated surface. (d) Characterization of MSNs by BET N_2 adsorption–desorption isotherms of as-synthesized MSNs and MSN-NGF. The surface area (S_{BET}), pore size (W_{BJH}), and pore volume (V_t) were measured using Brunauer–Emmett–Teller (BET) and Barrett–Joyner–Halenda (BJH) methods. The particle size was estimated by dynamic light scattering in deionized (DI) water.

observed and photographed using phase contrast microscopy (Nikon Diaphot).

2.10. Electrical stimulation

PC 12 cell neurite extension as a result of NGF release was accelerated by electrical stimulation. Ppy substrates were placed in borosilicate coverglass chambers consisting of three electrodes, a reference electrode (Ag/AgCl), a counter electrode (Pt), and a working electrode (Ppy film). The Ppy films upon which PC 12 cells were grown were stimulated with a current of 0.6 mA for 0.5–1 h to induce a burst release effect from the composite in response to continuous electrical stimulation. The analysis of neurite length was conducted after one day of stimulation. All experiments were performed in triplicate.

2.11. Statistical analysis

Unless otherwise specified, the unpaired student's t test (for comparison of two groups) or one-way ANOVA and Post Hoc Newman Keul's test (for more than two groups) were used for statistical analyses (InStat software). Normality was tested for by the Shapiro–Wilk test (STATA). Equal variances were tested by the method of Barlett for $n \geqslant 5$ (InStat), and by less than a two-fold difference in standard deviation (SD) for $n < 5$. Results are expressed as the mean ± SD. $P < 0.05$ was considered statistically significant.

3. Results and discussion

3.1. Incorporation of NGF into the pores of MSNs

MSNs synthesized with large-pore diameters have attracted much attention as an inorganic host material to encapsulate large biomolecules, such as enzymes, proteins, and even cells [22, 36–40]. The adsorption of substances by an inorganic matrix improves their stability by protecting them from the systematic circulation and consequently increases the therapeutic effect. MSNs possess some inherent advantages such as their nontoxic and biocompatible nature, adjustable pore size, large surface-to-volume ratio, and chemical stability with tunable degradation rates [37, 39–42].

As illustrated in figure 1(a), the encapsulation of NGF (MW 13 000) into the well-ordered internal structure of an MSN was performed by favorable electrostatic interaction

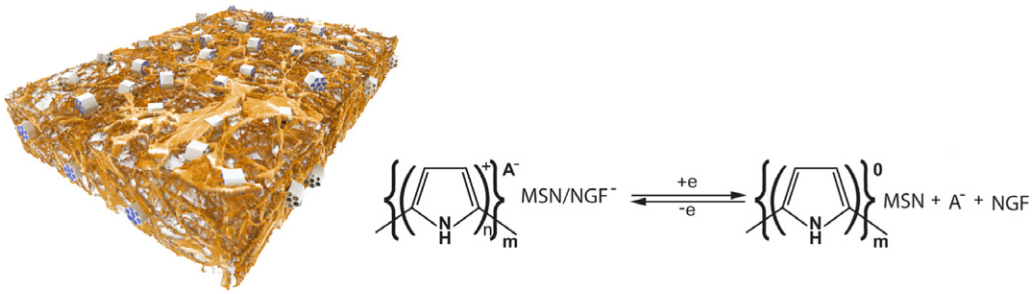

Figure 2. This illustration shows the colloidal particle assembled with electroactive polymers. The three electrode cells were used for electrochemical fabrication to achieve the incorporation of MSN-NGF as a co-dopant through the interaction with dopant anion, PSS (A^-). With a constantly applied electrical potential, NGF is released by redox cycling from the Ppy/MSN-NGF composite.

between free silanol groups on the wall of pore and positively charged amine groups of NGF at pH 7.0. The confinement of NGF to the MSN matrix was confirmed by TEM, N_2 adsorption, and XPS. As-synthesized CTAB-removed MSNs exhibit well-ordered pore structure with uniform mesopores (figure 1(b)) whereas NGF-loaded MSNs demonstrated filling, indicated by the presence of NGF inside the pore channels (figure 1(c)) [37, 43]. The incorporation of NGF is further highlighted by the comparison of the physical properties of as-synthesized MSN and MSN-NGF using a N_2 adsorption/desorption isotherm (figure 1 (d)). The BET test revealed 1040 $m^2\ g^{-1}$ surface area and 1.93 $cm^3\ g^{-1}$ of total pore volume of as-synthesized MSN with 4.71 nm of pore diameter. This indicated that MSNs possess enough space for drug molecules. The marked uptake of NGF lowered the surface area and total pore volume by approximately 60% and 80% respectively. Moreover, the reduction in average pore diameter strongly suggests that the majority of the pore walls were covered with NGF molecules. The particle size of MSN in PBS was measured by dynamic light scattering. Two different diameter distributions were observed: 101 and 125 nm corresponding to before and after NGF uptake respectively with approximately 31.5% of NGF encapsulation efficiency.

3.2. Synthesis and characterization of Ppy/MSN-NGF

The exogenous delivery of NGF to a lesioned area has been extensively investigated to enhance neural survival, outgrowth, and consequently nerve fiber regeneration as a potential therapeutic treatment for injury to the nervous system [44–46]. In general, the desired effectiveness is directly related to the performance of the drug after delivery to the site of action. To date, the lack of fine control of NGF application has become an impediment to therapeutic efficacy, and is often accompanied with unacceptable levels of abnormal nerve fiber sprouting [47, 48]. In addition, inherent short-lived NGF survival requires sustained and controllable release over a long period of time [49]. These practical problems would be helped by particulated delivery systems characterized by a prolonged and controlled release of sufficient amounts of NGF, while retaining its bioavailability. Meanwhile, it is well documented that the stimulation of peripheral and central nervous systems by continuous electrical pulses improves a neuronal deficit. The facilitation of nerve regeneration induced by the combination of a silica nanoparticle-based drug delivery system and electroactive polymer has the following advantages over conventional use. (1) Nanoparticles that are drug carriers possess a large surface area, which means concentrated amounts of the drug can be incorporated into the particle and can be triggered to be released at a controlled rate [50, 51]. MSNs as a drug delivery carrier have demonstrated their biocompatibility and nontoxicity [39, 40]. In addition, the drug entity can be safely protected during transportation. (2) The development of nanostructured surfaces with increased surface roughness has meant that these surfaces are more compatible with many cells by facilitating cellular attachment. In general, porous Si surfaces significantly enhance cell activity rather than a solid Si surface [52, 53]. Currently, the development of silica-based clinical applications to neurology have been extensively investigated including functionalized electrodes for stimulating and recording, to alleviate the symptoms of Parkinson's disease, visual and auditory assistive technology, and pain relief. The *in vivo* studies have demonstrated the biocompatibility and non-degradability of a PPy-coated surface which emphasizes the potential of PPy as a platform suitable for cell adhesion and subsequent cell proliferation [54, 55]. As a result, the functional silica-based conducting polymer surface offers much promise over that of conventional NGF therapy.

Polypyrrole (Ppy) films allow oxidative electrochemical polymerization. The inherent properties of electroactive polymers enable them to incorporate and subsequently release a diversity of biomolecules through repeating oxidation and reduction (redox) processes, where the polymer entraps anionic or cationic drugs in the oxidized state whereas it releases drugs when it is reduced to the neutral state. First, we verified feasibility using previously documented strategies. MSN-NGF incorporated polypyrrole (Ppy/MSN-NGF) films were synthesized during the polymerization process, where negatively charged MSN-NGF served as a co-dopant, as shown in figure 2. The sedimentation of silica particles was not observed during short electrochemical deposition ($\leqslant$1 m), demonstrating their stable dispersion in aqueous pyrrole solution.

It was evident that the entrapment of MSN-NGF within Ppy can be achieved with the aid of a dopant anion (PSS). Upon immobilization, we characterized each surface using:

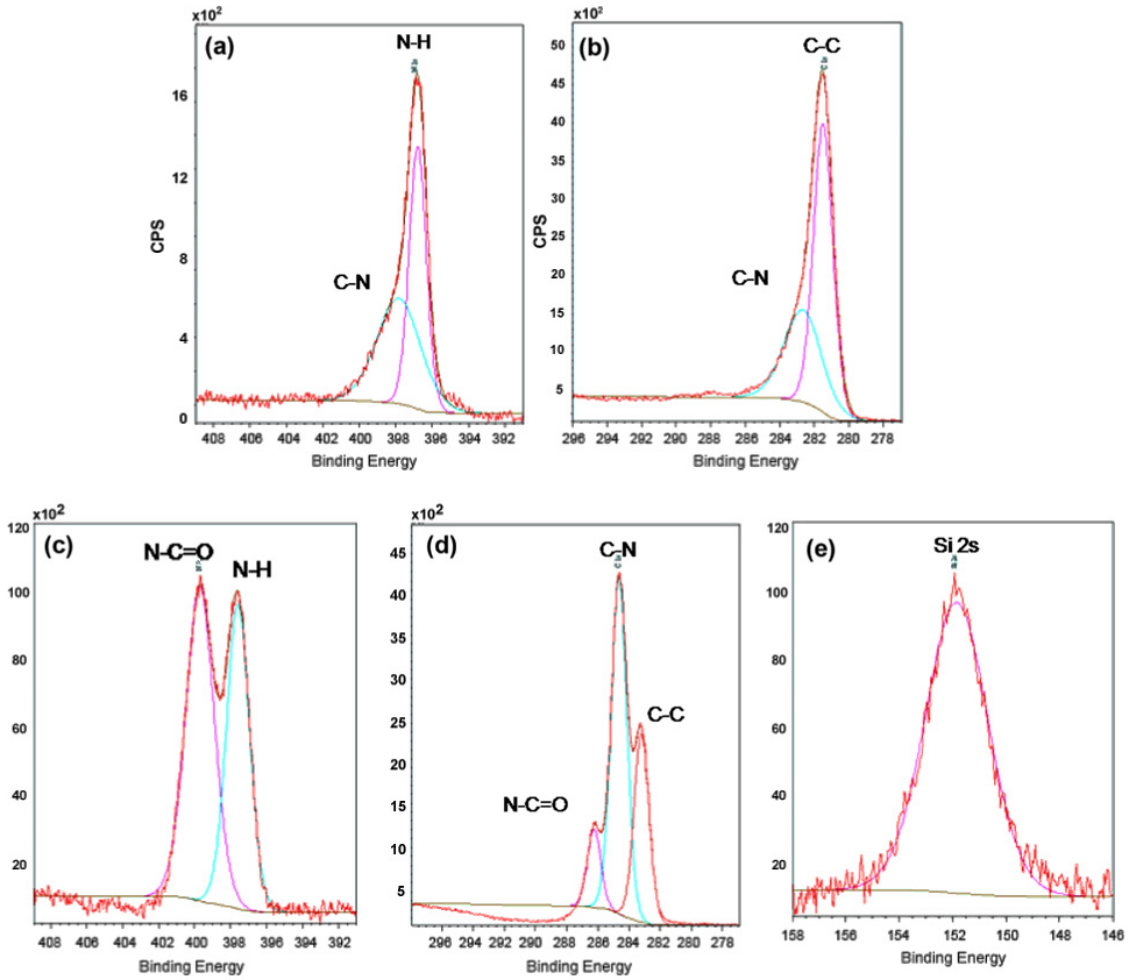

Figure 3. High resolution XPS for surface deconvolution analysis of (a) N 1s and (b) C 1s spectra of 'as-prepared' Ppy film, (c) N 1s, (d) C 1s, and (e) Si 2s spectra of a Ppy/MSN-NGF composite. The Si peak was not observed on the surface of Ppy.

(1) XPS to assess surface chemical functionality, (2) AFM and SEM for surface morphology, and (3) profilometry for film thickness. High resolution XPS was employed to characterize the chemical nature of the surface and to quantify surface changes after immobilization of MSN-NGF. It is important to know the presence of the main core-level peaks of silica, carbon, and nitrogen to understand the structure of these species present on the surface. Due to the broadness of peaks, the high resolution data were deconvoluted by commercially available software, as shown in figure 3.

The N 1s spectra of Ppy surfaces exhibit two distinct peaks at 397.0 and 398.5 eV corresponding to N–H and C–N, respectively (figure 3(a)). Once MSN-NGF was immobilized within Ppy, the high resolution N 1s spectra exhibited another predominant shoulder corresponding to amide-N (401.0 eV), as shown in figure 3(c). The appearance of amide peaks can be attributed to functionalization of the polymer surface with NGF. As expected, the C 1s spectra following MSN-NGF incorporation showed various functionalities such as C–C, C–N, and amide-C (figure 3(d)). A notable difference between 'as-prepared' Ppy and Ppy/MSN-NGF was the increase in the C–N species and the appearance of shouldering of the amide-C at 287.0 eV, which further confirmed the presence of NGF. Particularly, direct evidence that MSN-NGF is present within the Ppy can be confirmed by the existence of the Si 2s peak in the composite (figure 3(e)). These results proved the development of a composite film consisting of Ppy polymer and MSN-NGF, maintaining its conductivity and electroactivity. Figure 4(a) shows the effect of particle concentration on electrical conductivity.

As-prepared Ppy film showed an average specific conductivity of 9 S cm^{-1} obtained from ten measurements. As would be expected, the conductivity of Ppy films embedded with MSN-NGF decreased as a function of the increase in insulating behavior associated with the increase in concentration of MSNs. In consideration of the contact resistance during conductivity measurements (as most particles were located on the surface), the reduction in conductivity was reasonable. These observations were consistent with previous studies showing that the low conductivity of doped Ppy films is typical [32]. To determine the electroactivity of functionalized films, cyclic voltammograms (CV) were obtained in 0.2 M KCl at room temperature. In spite of the insulating nature of the particles, CV confirmed that functionalized Ppy composites possessed a significant increase in the electrochemical response associated with the

(a)

	Conductivity (S/cm)	Thickness (μm)
Ppy	8.98 ± 1.25	1.05 ± 0.22
Ppy/MSN-NGF With 0.1% nanoparticles	6.23 ± 1.08	1.8 ± 0.58
Ppy/MSN-NGF With 0.5 % nanoparticles	4.87 ± 0.50	–
Ppy/MSN-NGF With 1.0 % nanoparticles	4.01 ± 0.84	1.4 ± 0.37

(b)

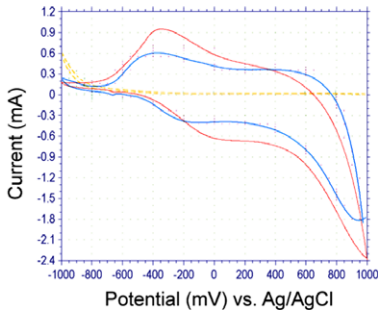

Figure 4. (a) Summary of conductivity and thickness of 'as-prepared' Ppy and particle-treated Ppy surfaces. The conductivity and thickness are dependent on the variation of concentration of the particles. (b) Cyclic voltammograms of the ITO substrate (dotted line), Ppy/MSN (red solid line), and Ppy/MSN-NGF (blue solid line) recorded in 0.2 M KCl at a scan rate of 100 mV s^{-1}. The insulating effect of particles reveals the lowered conductivity while they do not deteriorate the electroactivity of the surface.

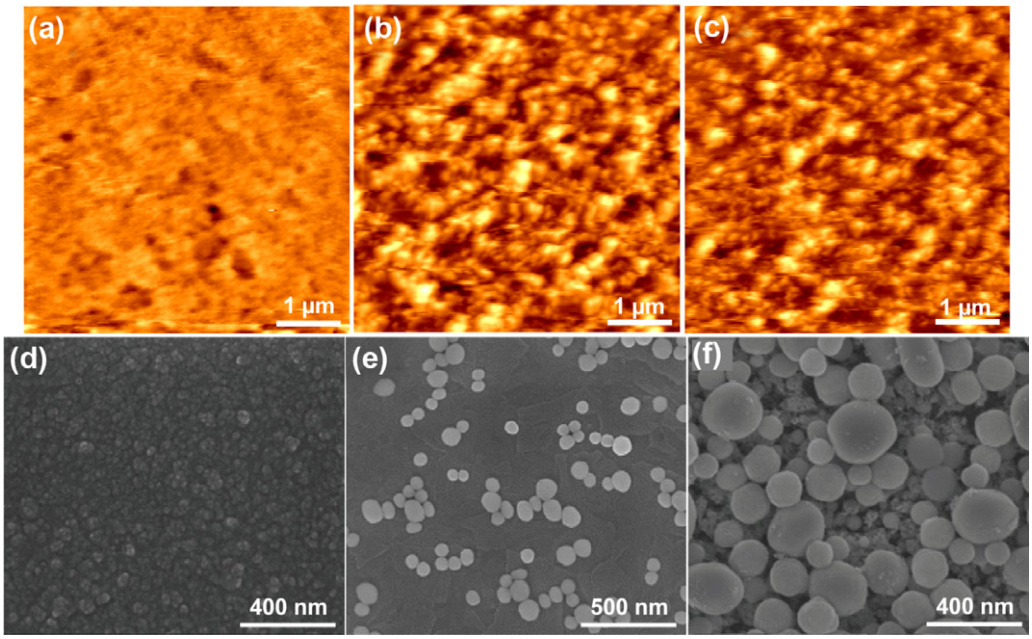

Figure 5. AFM topographical images of 5 μm by a 5 μm scan of (a) Ppy, (b) Ppy/MSN, and (c) Ppy/MSN-NGF. The incorporation of MSN significantly increased the surface roughness. SEM images of (d), 'as-prepared' Ppy, (e) Ppy film encapsulating MSN-NGF electrodeposited from suspension (0.1% MSN-NGF) for 50 s, and (F) Ppy film encapsulating MSN-NGF electrodeposited from suspension (1.0% MSN-NGF) for 200 s.

accumulated charge capacity as compared to bare ITO film (figure 4(b)). The surface topography after the immobilization reaction was evaluated by tapping-mode AFM obtained in air (figures 5(a)–(c)).

The 'as-prepared' Ppy film showed a relatively smooth surface with a surface roughness (rms) value of 22.52 nm. Upon the adsorption of particles, the rms value significantly increased, where rms values of 180.65 and 184.25 nm were recorded for Ppy/MSN and Ppy/MSN-NGF surfaces, respectively. Such a significant increase in the surface roughness indicates the presence of nanoparticles with a uniformly distributed spherical structure. SEM images further confirmed the AFM observations. As shown in figure 5(d), SEM images also revealed the appearance of randomly distributed globular features, or grains, located on the Ppy surface. These observations are consistent with previous reports that electrodeposition results in the evolution of characteristic 'cauliflower' features because the developing morphology is relatively governed by the nodular fractal type of growth of Ppy polymers—and uniformly observed over the entire surface [2, 56]. Ppy films incorporated with MSN-NGF also revealed the existence of a great number of fine solid particles which were completely different from the fluffy round shapes observed on 'as-synthesized' Ppy films, shown in figures 5(e) and (f). Such a uniform-sized, particle assembled structure re-emphasizes the presence of silica already confirmed by elemental analysis through XPS. Figures 5(e) and (f) are a more detailed view of the silica particles distribution within the Ppy film. The diameter of embedded particles was slightly increased, probably due

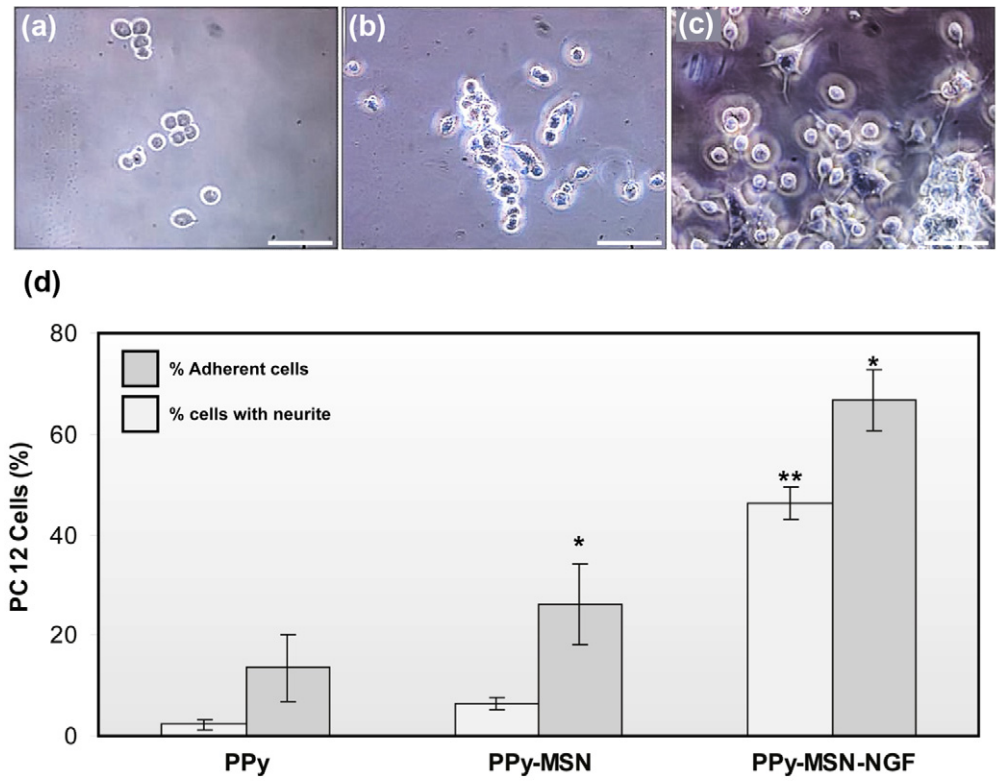

Figure 6. Phase contrast photomicrographs of PC 12 cell cultured on (a) Ppy film, (b) Ppy/MSN, and (c) Ppy/MSN-NGF. The scale bar represents 50 μm. All images were taken at the same magnification. (d) Quantification of cells adhered to each surface and the % of the cell population with neurite outgrowth. The high population of cells on Ppy/MSN-NGF composite is attributed to the local delivery of NGF. $^{*}P < 0.01, ^{**}P < 0.05$.

to the effect of a continuous polypyrrole coating around individual particles or particle aggregations. During film growth, the surface coverage of particles is governed by both the concentration of particles and the deposition time. At the same electrical potential, a random and loosely distributed array of MSN-NGF on the surface of Ppy was observed when 0.1% nanoparticles were suspended in the electrolyte solution and deposited for 50 s, see figure 5(e). On the other hand, more particles were deposited within the Ppy film as closely-packed layers when the deposition time and particle concentration were increased to 300 s and 1% respectively, as shown in figure 5(f).

The assembly of nanoparticles generates a nonplanar topography which offers a favorable environment for biomolecules or cell attachment by preserving physicochemical surface properties. Evidently, these electrochemical investigations suggest a strong interaction between Ppy and MSN-NGF and suggest further investigations of the interaction between living cells and the Ppy/MSN-NGF composite. To this end, we cultured PC 12 cells on electrochemically deposited surface environments of Ppy, Ppy/MSN, and Ppy/MSN-NGF to observe the pattern of spreading and neurite extension from PC 12 cells after two days in culture (figure 6).

To study cellular behavior, Ppy/MSN-NGF composites with closely packed arrays were used. PC 12 cells showed better cell adhesion and spreading on Ppy/MSN and Ppy/MSN-NGF than 'as-prepared' Ppy. Enhanced cellular activity would be expected on these former surfaces by recognizing the nonplanar surface that is created by the assembly of MSN-NGF. Many types of cells preferentially respond to the micro-or nanoparticle assembled surfaces composed of various surface features such as grooves or ridges. Cellular response and morphology show high affinity as a function of the density of monolayered particles; on the monolayer composed of closely packed particles, the average spread of cells and their processes is more stable than that of cells applied to loosely packed particles [57]. Said another way, the more dispersed particles are likely to inhibit strong adhesion and may provide even more subtle influence over many aspects of integrin behavior responsible for cell adhesion and morphology. By tailoring the inter-particle space, colloid-based arrays can be constructed as a convenient three-dimensional structure for cell–surface interaction. Such a colloidal particle assembly demonstrates the ability to modulate cellular functions and to guide specific cell responses. Here, the cells grown on Ppy, Ppy/MSN, and Ppy/MSN-NGF exhibited significantly different morphological features. The cells grown on 'as-prepared' Ppy did not show obvious neurite outgrowth see figure 6(a). In contrast, figure 6(c) shows extensive neurite outgrowth, multiple neurite extensions, and the contact of adjacent cells, suggesting that nanoscaled Ppy/MSN-NGF composites triggered increased neuronal activity through a supply of NGF. Figure 6(d) quantifies the cell population attached to each type of surface, and the percentage of cells with neurite extensions. With a negligible probability of neurite extension, cells were rounded and weakly adhered to

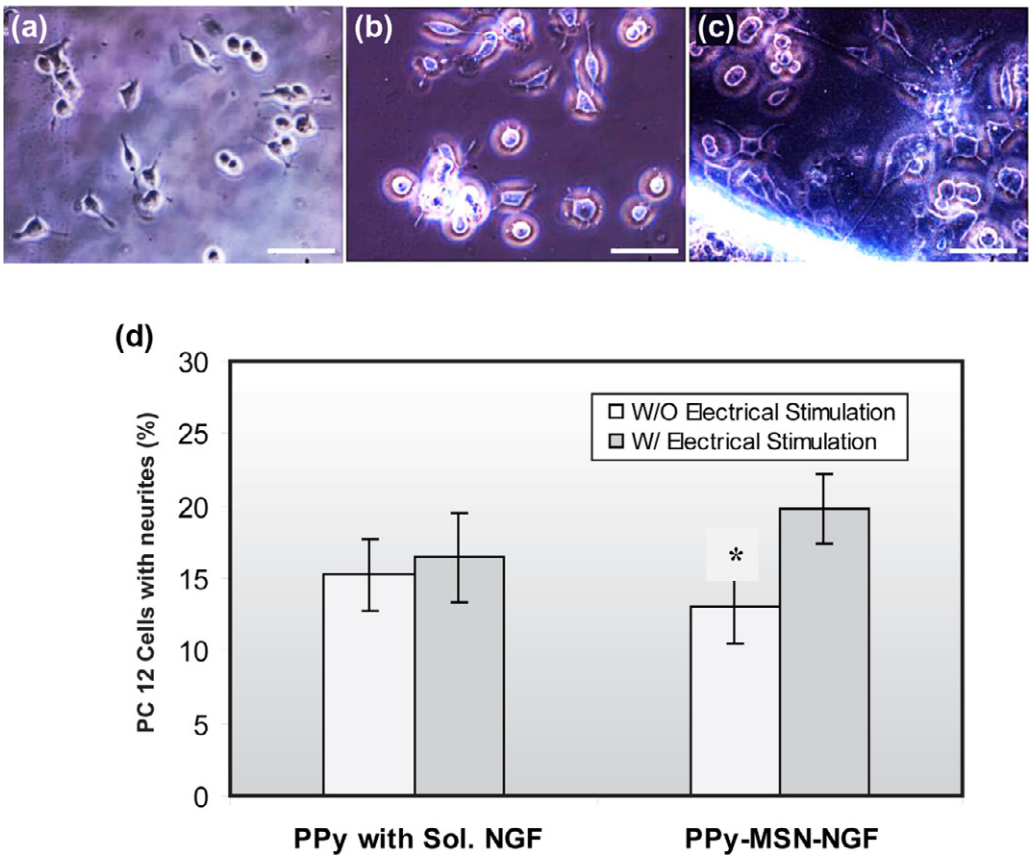

Figure 7. Phase contrast images of PC 12 neurite extension after two days in culture. (a) Cells grown on Ppy film with NGF solution (50 ng ml^{-1}) in the culture medium. (b) The cells cultured on unstimulated Ppy/MSN-NGF film. (c) The cells cultured on stimulated Ppy/MSN-NGF film. (d) Quantification of neurite extension data represented in (a) through (c). Electrically conductive surfaces initiate a cellular response that influences adhesion, proliferation, and neurite extension. $^{*}P < 0.05$.

the film surface when placed in contact with the surface of 'as-prepared' Ppy. The weak binding of cells to this surface is direct evidence of reduced proliferation because cell adhesion and spreading is a prerequisite for cell cycle division. On the other hand, Ppy/MSN composites exhibited enhanced cell spreading and morphology, suggesting cells could not only recognize the topographical character of the surface, but could also respond to it. Approximately 67% of those cells grown on Ppy/MSN-NGF adhered well to it and approximately 48% of these possessed neurite extensions.

3.3. Release of NGF from Ppy/MSN-NGF with or without electrical stimulation

Here, we have confirmed the bioactivity of NGF released from Ppy/MSN-NGF composites. In particular, it was apparent that a colloid-based array was associated with the variation in cell adhesion and proliferation, even in the absence of NGF. But when NGF was encapsulated within the composite, direct delivery of NGF to the local area was accomplished and cell growth with enhanced neurite sprouting was encouraged. In this application, NGF-absorbed surfaces combined with a subthreshold electrical potential significantly released this growth factor in response to electrical stimulation. The extensive influence on neural growth by applying steady DC electric fields has been investigated and directed at improving functional recovery in the nervous system [58, 59]. We wished to use an electrical potential to trigger higher levels of NGF release into the extracellular space. In order to examine the effectiveness of electrical stimulation, a solution of NGF (50 ng ml^{-1}) was added to the medium of control Ppy surface and adhered cells were observed 24 h after the treatment. A statistically significant difference between the values of neurite extensions of cell grown on 'as-prepared' Ppy surfaces was not achieved ($P < 0.05$, figure 7(a)).

However, cells grown on electrically stimulated Ppy/MSN-NGF composite showed a statistically significant increase in the amount of neurite extension and growth compared to nerve cells cultured without electrical stimulation. This suggested that subsequent electrical stimulation resulted in elevated release levels of NGF shown in figure 7(c). The effect of electrical stimulation induces an approximately 40% increase in the cell population possessing neurite extensions. The contraction and expansion process of Ppy in response to electrical stimulation enhanced the release of NGF from individual MSN-NGF coated with Ppy. The controlled-release profile of NGF from Ppy/MSN-NGF composites was examined with consideration of the electrical stimulation (figure 8(a)).

NGF release behavior showed linear enhancement as the concentration of MSN-NGF embedded in Ppy film increased.

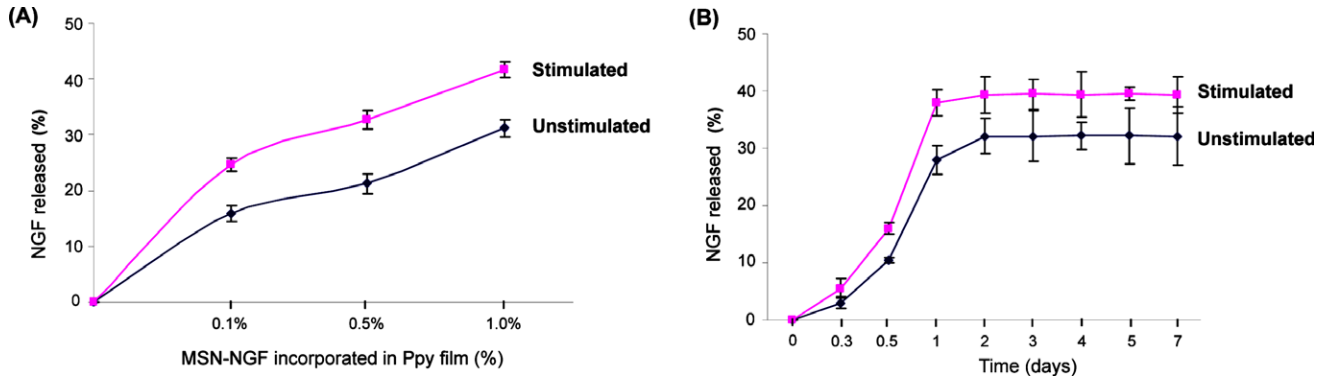

Figure 8. (a) The release profile of NGF from unstimulated and stimulated Ppy/MSN-NGF for two days as a function of concentration of MSN-NGF. (b) The cumulative NGF release over a week from Ppy/MSN-NGF composite in the presence or absence of electrical stimulation.

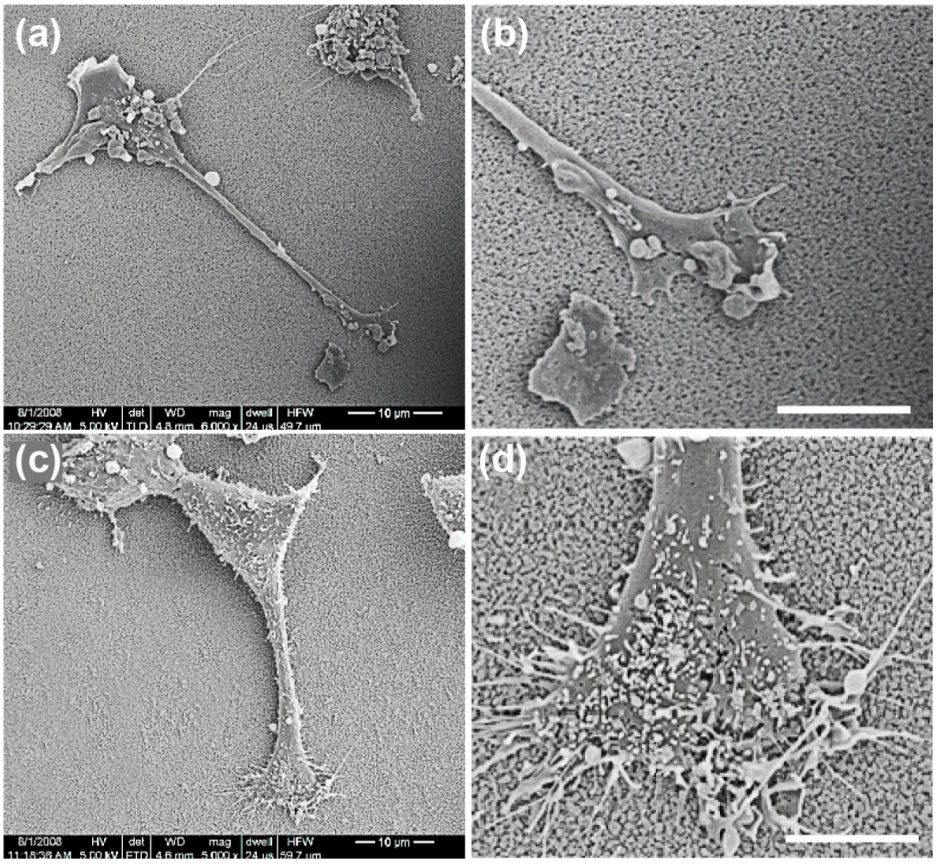

Figure 9. SEM images of cells and neurites grown on unstimulated Ppy/MSN-NGF (a) and (b) and electrically stimulated surfaces (c) and (d). The scale bar represents 20 μm (b) and 10 μm (d). The cells cultured on stimulated Ppy/MSN-NGF show growth cone formation, neurite extension, and significant microspike formation.

In all experiments, the effect of stimulation with a constant current density of 0.6 mA cm^{-2} caused almost two times greater NGF release than that leakage from unstimulated films. This result is consistent with previous studies, where electrostatic interaction produced by electrical stimulation is critical to the release mechanism [31, 60, 61]. We also assessed the cumulative release of NGF over one week, as shown in figure 8(b). Interestingly, the majority of NGF release was reached in the first 24 h and then plateaued at this level for the next 6 days. The amount of NGF released apparently depends on the initial concentration that was loaded. Such a 'burst release' trend was also investigated after the application of electrical stimulation. This release pattern showed a similar scenario to the study of Thompson *et al*, where the prolonged and sustained release of neurotrophin-3 (NT-3) following the initial burst would cooperate to promote cell signaling in the localized area and facilitate local biochemical processes and cellular responses [2]. To further investigate the interaction between PC 12 cells and Ppy/MSN-NGF, SEM images revealed enhanced attachment and neurite extensions, as shown in figure 9.

Low-magnification images from stimulated and unstimulated surfaces were indistinguishable. The cells plated on both surfaces possessed long neurites approximately 20 μm in length after two days in culture. However, higher-magnification SEM images detailed distinguishable differences in the morphology and shape of cells. The formation of growth cones on the stimulated Ppy/MSN-NGF composite showed significant filopodial and microspike extensions which drive neurite outgrowth, shown in figure 9(d) [62]. Such macro-and micro-extensions of the growth cone membrane were not characteristic of cells grown on unstimulated film. The strong interaction between extended neurites and custom-made composite surfaces suggests nanoscaled composites might be ideal as a permissive substrate for nerve fiber survival and growth. Furthermore, long-term local delivery of NGF via electrically activated Ppy/MSN-NGF composites would enhance the usefulness of these substrates since cytokine-stimulated cellular activity could be chosen in time and thus adapted to the local environment of implantation sites.

4. Conclusions

In this study, NGF-loaded mesoporous silica nanoparticles, or MSN-NGF, were electrochemically deposited within Ppy film. The amount of incorporated particles was optimized using a correlation between the concentration of particles and the electrodeposition time. Particles with treated surfaces were capable of a controlled release of a neuronal growth factor which induced specific cellular responses in target PC 12 cells. PC 12 cells exhibited significant enhancement of attachment, spreading, and proliferation behavior on Ppy/MSN-NGF, or even Ppy/MSN surfaces, when compared with 'as-prepared' Ppy films. Some of these responses can be attributed to the effect of nonplanar surfaces on adhered cells in concert with the enhancement produced by growth factor delivery. The release profile of NGF was linearly related to the loading concentration. An initial large release was followed by a phase of continuous and stable release. This was observed in both stimulated and unstimulated Ppy/MSN-NGF surfaces. Cells plated on electrically stimulated surfaces were more likely to produce an enhanced attachment, and show neurites and growth cone extensions possessing a more active appearance.

Acknowledgments

We gratefully thank Judy Grimmer for her expertise and help with *in vitro* cell culture. We appreciate the excellent illustrations and graphics of Michel Schweinsberg, and financial support from the General Funds of the Center for Paralysis Research, The State of Indiana, and a generous endowment from Mrs Mari Hulman George.

References

[1] Cui X Y, Wiler J, Dzaman M, Altschuler R A and Martin D 2003 *Biomaterials* **24** 777–87
[2] Thompson B, Moulton S, Ding J, Richardson R, Cameron A, O'Leary S, Wallace G and Clark G 2006 *J. Control. Release* **116** 285–94
[3] Wallace G and Kane-Maguire L 2002 *Adv. Mater.* **14** 953–60
[4] Willerth S and Sakiyama-Elbert S 2007 *Adv. Drug Deliv. Rev.* **59** 325–38
[5] Wise K D and Najafi K 1991 *Science* **254** 1335–42
[6] Frampton J P, Hynd M R, Willams J C, Shuler M L and Shain W 2007 *J. Neural Eng.* **4** 399–409
[7] Schwartz A B, Cui X T, Weber D J and Moran D W 2006 *Neuron* **52** 205–20
[8] Stieglitz T 2007 *Acta Neurochir. Suppl.* **97** 411–8
[9] Pernaut J M and Reynolds J R 2000 *J. Phys. Chem.* B **104** 4080–90
[10] Richardson R T, Thompson B, Moulton S, Newbold C, Lum M, Cameron A, Wallace G, Kapsa R, Clark G and O'Leary S 2007 *Biomaterials* **28** 513–23
[11] Wadhwa R, Carl L and Xinyan C 2006 *J. Control. Release* **110** 531–41
[12] Wang X, Gu X, Yuan C, Chen S, Zhang P, Zhang T, Yao J, Chen F and Chen G 2004 *J. Biomed. Mater. Res.* A **1** 411–22
[13] Cen L, Neoh K G and Kang E T 2002 *Langmuir* **18** 8633–40
[14] Collier J H, Camp J P, Hudson T W and Schmidt C E 2000 *J. Biomed. Mater. Res.* **50** 574–84
[15] Gomez N and Schmidt C E 2007 *J. Biomed. Mater. Res.* A **81** 135–49
[16] Li Y, Neoh K G and Kang E T 2005 *J. Biomed. Mater. Res.* A **73** 171–81
[17] Sanghvi A B, Miller K P, Belcher A M and Schmidt C E 2005 *Nat. Mater.* **4** 496–502
[18] Brannon-Peppas L and Blanchette J O 2004 *Adv. Drug. Deliv. Rev.* **56** 1649–59
[19] Downing G 2005 *Science* **310** 1132–4
[20] Duncan R 2003 *Nat. Rev. Drug Discovery* **2** 347–60
[21] Emerich D F and Thanos C G 2006 *Biomol. Eng.* **23** 171–84
[22] Jin S and Ye K 2007 *Biotechnol. Prog.* **23** 32–41
[23] Liu Y, Miyoshi H and Nakamura M 2007 *Int. J. Cancer* **120** 2527–37
[24] Rhyner M, Smith A, Gao X, Mao H, Yang L and Nie S 2006 *Nanomedicine* **1** 1–9
[25] Chen G, Wang Z, Yang T, Huang D and Xia D 2006 *J. Phys. Chem.* B **110** 4863–8
[26] Hepel M 1998 *J. Electroanal. Chem.* **145** 124–34
[27] Kulesza P J, Chojak M, Karnicka K, Miecznikowski K, Palys B and Lewera A 2004 *Chem. Mater.* **16** 4128–34
[28] Xu P, Han X, Wang C, Zhao H, Wang J, Wang X and Zhang B 2008 *J. Phys. Chem.* B **112** 2775–81
[29] Marini M, Pilati F and Pourabbas B 2008 *Macromol. Chem. Phys.* **209** 1374–80
[30] Ateh D D, Navsaria H A and Vadgama P 2006 *J. R. Soc. Interface* **3** 741–52
[31] Guimard N K, Gomez N and Schmidt C E 2007 *Prog. Polym. Sci.* **32** 876–921
[32] Gomez N and Schmidt C E 2006 *J. Biomed. Mater. Res.* A **81** 135–49
[33] Richardson-Burns S, Hendricks J L and Martin D C 2007 *J. Neural Eng.* **4** L6–13
[34] Wallace G and Spinks G 2007 *Soft Matter* **3** 665–71
[35] Slowing I, Trewyn B and Lin V 2007 *J. Am. Chem. Soc.* **129** 8845–9
[36] Andersson J, Rosenholm J, Areva S and Linden M 2004 *Chem. Mater.* **16** 4160–7
[37] Balas F, Manzano M, Horcajada P and Vallet-Regi M 2006 *J. Am. Chem. Soc.* **128** 8116–7
[38] Chung T, Wu S, Yao M, Lu C, Lin Y, Hung Y, Mou C, Chen Y and Hyang D 2007 *Biomaterials* **28** 2959–66
[39] Lai C Y, Trewyn B G, Jeftinija D M, Jeftinija K, Xu S, Jeftinija S and Lin V S 2003 *J. Am. Chem. Soc.* **125** 4451–9
[40] Munoz B, Ramila A, Perez-Pariente J, Diaz I and Vallet-Regi M 2003 *Chem. Mater.* **15** 500–3
[41] Trewyn B, Slowing I, Giri W, Chen H and Lin V 2007 *Acc. Chem. Res.* **40** 846–53

[42] Wang L, Wang K, Santra S, Zhao X, Hilliard L, Smith J, Wu Y and Tan W 2006 *Anal. Chem.* **78** 646–54
[43] Lin Y, Hung Y, Su J, Lee R, Chang C, Lin M and Mou C 2004 *J. Phys. Chem.* B **108** 15608–11
[44] Mahoney M and Saltzman W 2001 *Nat. Biotechnol.* **19** 934–9
[45] Murakami Y, Furukawa S, Nitta A and Furukawa Y 2002 *J. Neurol. Sci.* **198** 63–9
[46] Thuret S, Moon L and Gage F 2006 *Nat. Rev. Neurosci.* **7** 628–43
[47] Lambias A, Ramp P, Bonini S, Caprioglio G and Aloe L 1998 *New Engl. J. Med.* **338** 1174–80
[48] Schwab M 2002 *Science* **295** 1029–31
[49] Gillespie L N, Clark G M, Barlett P F and Marzella P L 2003 *J. Neurosci. Res.* **71** 785–90
[50] Ahmed A, Bonner C and Desai T A 2002 *J. Control. Release* **81** 291–306
[51] Tao S L and Desai T A 2003 *Adv. Drug Deliv. Rev.* **55** 315–28
[52] Bayliss S C, Bucberry L D, Fletcher I and Tobin M J 1999 *Sensors Actuators* A **74** 139–42
[53] Fan Y W, Cui F Z, Hou S P, Xu X Y, Chen L N and Lee I S 2002 *J. Neurosci. Met.* **120** 17–23
[54] Wang X, Gu X, Yuan C, Chen S, Zhang P, Zhang T, Yao J, Chen F and Chen G 2004 *J. Biomed. Mater. Res.* A **68** 411–22
[55] Williams R L and Doherty P J 1994 *J. Mater. Sci. Mater. Med.* **5** 429–33
[56] Fredja H B, Helalia S, Esseghaiera C, Vonnab L, Vidalb L and Abdelghani A 2007 *Tanlanta* **75** 740–7
[57] Gleason N J, Nodes C J, Higham E M, Guckert N, Aksay I A, Schwarzbauer J E and Carbeck J D 2003 *Langmuir* **19** 513–8
[58] Borgens R B 1999 *Neuroscience* **91** 251–64
[59] English A W, Schwartz G, Meador W, Sabatier M J and Mulligan A 2007 *Dev. Neurobiol.* **67** 158–72
[60] Geetha S, Chepuri R K, Rao M and Trivedi D C 2006 *Anal. Chim. Acta* **568** 119–25
[61] Kontturi K, Pentti P and Sundholm G 1998 *J. Electroanal. Chem.* **453** 231–8
[62] Dent E W *et al* 2007 *Nat. Cell Biol.* **9** 1347–59